Confinement-Induced Glassy Dynamics in a Model for Chromosome Organization

Hongsuk Kang,[1] Young-Gui Yoon,[2] D. Thirumalai,[1] and Changbong Hyeon[3,*]

[1]*Institute for Physical Sciences and Technology, University of Maryland, College Park, Maryland 20742, USA*
[2]*Department of Physics, Chung-Ang University, Seoul 156-756, Korea*
[3]*Korea Institute for Advanced Study, Seoul 130-722, Korea*

Recent experiments showing scaling of the intrachromosomal contact probability, $P(s) \sim s^{-1}$ with the genomic distance s, are interpreted to mean a self-similar fractal-like chromosome organization. However, scaling of $P(s)$ varies across organisms, requiring an explanation. We illustrate dynamical arrest in a highly confined space as a discriminating marker for genome organization, by modeling chromosomes inside a nucleus as a homopolymer confined to a sphere of varying sizes. Brownian dynamics simulations show that the chain dynamics slows down as the polymer volume fraction (ϕ) inside the confinement approaches a critical value ϕ_c. The universal value of $\phi_c^\infty \approx 0.44$ for a sufficiently long polymer ($N \gg 1$) allows us to discuss genome dynamics using ϕ as the sole parameter. Our study shows that the onset of glassy dynamics is the reason for the segregated chromosome organization in humans ($N \approx 3 \times 10^9$, $\phi \gtrsim \phi_c^\infty$), whereas chromosomes of budding yeast ($N \approx 10^8$, $\phi < \phi_c^\infty$) are equilibrated with no clear signature of such organization.

Chromosomes exhibit dramatic changes in their spatial organization along the cell cycle. In the metaphase, they are condensed into compact bloblike structures [1], whereas in the interphase they decondense to less compact coil-like structures. Interphase chromosomes are not random but form territories [2], and their organization may be fractal-like [3]. Advances in experimental techniques [3–7] have provided quantitative details of chromosome organization in the form of chromosomal contact maps describing how distant loci are structurally organized. The contact probability of two loci separated by a genomic distance s scales as $P(s) \sim s^{-1}$, differing from $P(s) \sim s^{-1.5}$ in equilibrated polymer melts. The deviation of the exponent from -1.5 is taken as evidence that chromosomes form a nonequilibrium globule with segregated domains rather than a fully equilibrated globule with entanglements [3,8]. Such an interpretation of the structural organization based solely on $P(s)$ is not universally accepted [9]. In addition, genome structure could vary depending on the extent of maturity of human cells [10]. Still, the scaling of $P(s)$ varies depending on organisms. It is therefore important to develop a theoretical framework for distinguishing between genome structures in different organisms.

From a biological perspective, it could be argued that the hierarchical and scale-free organization of chromosome, without knots, is beneficial for access to a target locus [11] or for the faster response to an environmental change by easing the condensation-decondensation process [12,13]. Although the origin of chromosomal territories is controversial because equilibrium polymer configurations with many loops naturally produce segregated domains as well [14,15], a major nonequilibrium effect, glassy dynamics of

the genome under strong confinement, should not be overlooked as a contributing factor in chromosome folding. The relaxation time of a polymer via disentanglement [16] ($\tau_{\text{rep}} \sim N^3$ [12,13,17,18]) could be far longer, effectively permanent for higher organisms, than the cell cycle time (τ_{cell}) [12,13] for a large N. Furthermore, a substantial increase of polymer relaxation time is also expected in a strong confinement as is the case for DNA inside a viral capsid [19] even when N is not too large. Thus, to fully describe the genome structuring, it is imperative to understand the polymer dynamics under confinement and how it might vary across various species. The major goal of this work is to develop a physical basis, using relaxation dynamics as a quantitative measure, to discriminate between genome organization in different organisms.

Although explicit models that consider circular DNA or multichains and specific contacts based on Hi-C contact maps [20–22] are possible, here we study the dynamics of homopolymers confined to a sphere of varying sizes as a first step towards understanding the dynamical features of interphase chromosomes. We consider a single self-avoiding polymer chain, representing chromatin fiber, confined to a sphere and employ dynamical measures previously used to study supercooled liquids [23–25] as a vehicle to investigate nonequilibrium effects. Our major finding is that the dynamics and organization of the homopolymer vary dramatically as the extent of confinement is increased. When this result is translated into genome organization, we find that bacteria and yeast chromosome folding can be thought of as an equilibrium process whereas glassy behavior governs the territorial organization in humans. These inferences cannot be drawn from genome contact

maps alone, which has been the sole focus of chromosome folding.

The equilibrium aspects of confined polymers are well understood [17,26]. The equilibrium free energy of a polymer confined to a sphere is not extensive [27,28] in contrast to polymer localization in a slit or a cylinder. Furthermore, as the extent of confinement increases, the volume fraction, defined by $\phi = (R_g^c/R_s)^3$ (Fig. 1(a), see Supplemental Material [29]) increases, and more importantly, the equilibration time of the chain (τ_{eq}) increases dramatically. If τ_{eq} for a genome is longer than the finite cell doubling time (τ_{cell}) then the decondensation-condensation cycle dynamics of the genome should be under kinetic control. We explore these aspects in the context of genome folding using simulations of homopolymers confined in a sphere (see Supplemental Material [29] for details), highlighting the confinement effect on a polymer leading to the ultraslow glassy dynamics, such that $\tau_{eq} \gg \tau_{cell}$, which we will show is the case in human chromosomes ($N \approx 10^9$) and viral DNA ($N \approx 10^5$).

In general, it is difficult to distinguish between non-equilibrium conformation of a polymer and its equilibrium counterpart because polymer configurations for both cases could be similar, just as is the case for liquids and glasses. Indeed, the polymer size with increasing N satisfies the Flory relationship, $R_g \sim N^\nu$ with $\nu \approx 3/5$ and $1/3$ for weak and strong confinement, respectively [Fig. 1(b)], crossing

over the regime $R_g \sim N^{1/2}$ at $\phi^{(\theta)} \approx 0.2$ where repulsion due to excluded volume is counterbalanced by the confinement pressure. Therefore, in strong confinement R_g scaling cannot distinguish between equilibrium and nonequilibrium globules. The radial distribution function (RDF) between monomers at high ϕ is reminiscent of the closely packed structure [Fig. 1(c)], suggesting that extent of confinement controls the chain organization.

The scaling exponent α of the contact probability between two sites separated by the chain contour s, $P(s) \sim s^{-\alpha}$, is one way to assess the chain organization. (Alternatively, the average distance between two loci separated by s, $R(s) \sim s^\nu$, can be used [9,15], see Fig. S3.) $P(s) \sim s^{-2.18}$ is expected for unconfined self-avoiding walk (SAW) (see Supplemental Material [29]) [30–32]. For an equilibrium globule under strong confinement, polymer chains are in near Θ condition because of the effective cancellation between attraction and repulsion. Hence, we expect that $P(s) \sim s^{-\alpha}$ with $\alpha = 1.5$ [17,33]. In the case of strong confinement, however, $P(s) \sim s^{-1}$ in the range of $s/a \sim \mathcal{O}(10)$ for $N = 300$, similar to the scaling observed in the Hi-C analysis of the chromosome in interphase [3,34]. The range of s^{-1} scaling increases as the extent of confinement increases [Fig. 1(d)].

However, $P(s)$ scaling is not an indicator of the underlying dynamics. Even for a SAW chain with no specific attractive interaction, dynamics can be arrested in strong
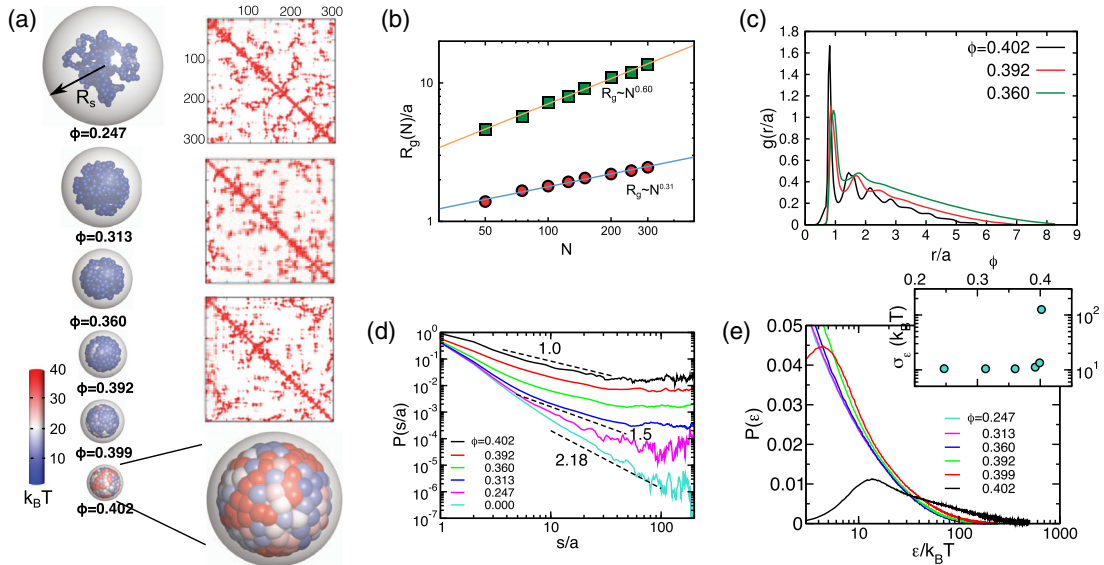

FIG. 1 (color online). Polymer ($N = 300$) confined to spheres. (a) Snapshots from simulations. The value of the potential energy (scale on the left) for each monomer shows that the spatial heterogeneity increases as ϕ approaches $\phi_c(300) \approx 0.404$ (see Fig. S5 for other snapshots). Contact maps from three distinct polymer configurations at $\phi = 0.402$ near $\phi_c(300)$ are shown on the right. (b) Flory laws $R_g \sim N^{3/5}$ and $\sim N^{1/3}$ are satisfied for unconfined and strongly confined ($\phi = 0.402$) chains of varying N, respectively. (c) RDFs (see Supplemental Material [29]) at three ϕ values. (d) Intersegmental contact probabilities (see Supplemental Material [29] for definition) with increasing ϕ from 0 to 0.404 ($N = 300$). (e) Distributions of monomer energy ($\epsilon_i = U_i^{bond} + \sum_{j\neq i} U_{i,j}^{ex}$, where the surface interaction term is excluded from the calculation. See Supplemental Material [29].), $P(\epsilon) = N^{-1} \sum_{i=1}^{N} \delta(\epsilon_i - \epsilon)$, for increasing ϕ. Divergence of the standard deviation [$\sigma_\epsilon^2 = \langle \epsilon^2 \rangle - \langle \epsilon \rangle^2$ where $\langle \epsilon^n \rangle = \int_0^\infty \epsilon^n P(\epsilon) d\epsilon$] near ϕ_c is shown in the inset.

confinement, preventing a full equilibration of the chains on relevant time scales. We document the emergence of glassy behavior under strong confinement by first calculating the potential energy of each monomer [Figs. 1(a), 1(e), S5]. The spatial heterogeneity of monomer energies at $\phi = 0.402$ is striking [Figs. 1(a), S5], which is also indicated by the abrupt changes in the monomer energy distribution $P(\epsilon)$ [Fig. 1(e)] and the standard deviation σ_ϵ [Fig. 1(e), inset].

In the absence of obvious symmetry breaking, it is useful to characterize the dynamics using the van Hove correlation function to discern the onset of glasslike behavior [23]. The correlation function,

$$F_{\vec{q}}(t) = \frac{1}{N} \sum_{j=1}^{N} e^{i\vec{q}\cdot[\vec{r}_j(t) - \vec{r}_j(0)]}, \tag{1}$$

provides dynamical information of how the system relaxes from its initial configuration, where $\vec{r}_j(t)$ is a position of jth monomer at time t. The ensemble-averaged isotropic self-intermediate scattering function $\langle F_q(t) \rangle$ is estimated by integrating $F_{\vec{q}}(t)$ over space with $q = |\vec{q}|$ and at $q = q_{\max} = 2\pi/r_s$, where r_s is the position of the first peak in the total pair distribution function [see Fig. 1(c)]. The onset of the structural glass transition is described by the density-density correlation function $\langle F_q(t) \rangle$ as a natural order parameter, which decays to zero in the liquid phase, but saturates to a nonzero value in the glassy phase even at long times. Thus, $\langle F_{q_{\max}}(t) \rangle$ provides information of how rapidly the polymer confined to a sphere loses memory of the initial configuration [Fig. 2(a)]. From physical considerations, $\langle F_{q_{\max}}(t) \rangle$ should vanish at long times ($t \to \infty$) for $\phi < \phi_c$; the decorrelation time of the polymer configuration increases sharply as the extent of confinement (or ϕ) approaches its dynamical arrest value. $\langle F_{q_{\max}}(t) \rangle$ at various ϕ is well fit by a stretched exponential function $\sim e^{-(t/\tau_\alpha)^\beta}$, and the dependence of τ_α on ϕ for different N (Fig. 2) is analyzed using the relation,

$$\tau_\alpha(\phi; N) = \tau_0(N)[\phi_c(N) - \phi]^{-\nu_\tau}. \tag{2}$$

The relaxation time $\tau_\alpha(\phi; N)$ increases with ϕ and diverges at $\phi_c(N)$. The stretching exponent β decreases with ϕ (Fig. S4), consistent with our findings in Fig. 1(a) that the system becomes more glassy as ϕ increases. The set of $\tau_\alpha(\phi; N)$, for various N, are described by a universal curve, satisfying $\log(\tau_\alpha/\tau_0) = -\nu_\tau \log[\phi_c(N) - \phi]$, and hence we obtain a universal scaling exponent $\nu_\tau \approx 0.65$ for the dynamical arrest. The critical volume fraction $\phi_c(N)$ is N dependent but saturates to a finite value ϕ_c^∞ in the limit $N \to \infty$. From finite size scaling [Fig. 2(c)], we obtain $\phi_c^\infty \approx 0.45$.

As an alternative to $\tau_\alpha(\phi)$, the fluctuations in $F_{q_{\max}}(t)$, namely the generalized susceptibility $\chi_4(t)$ corresponding
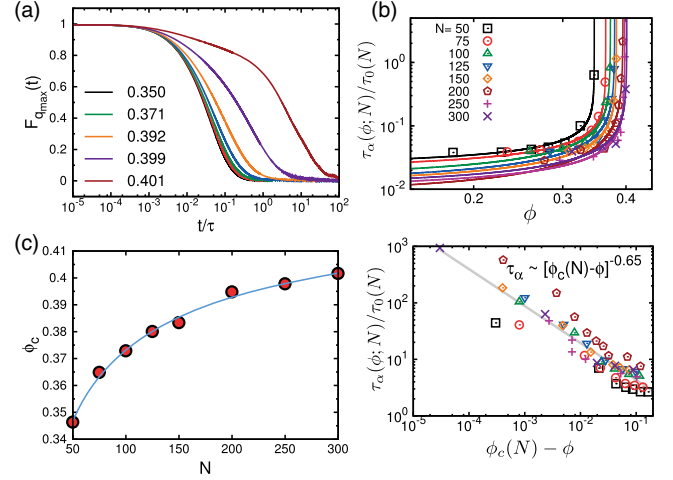

FIG. 2 (color online). Polymer dynamics under confinement probed using $\tau_\alpha(\phi)$. (a) $\langle F_{q_{\max}}(t) \rangle$ with varying ϕ for $N = 300$. The time on the abscissa is scaled by $\tau = a^2/D$ (see Supplemental Material [29]). (b) (top) For a polymer with N, $\tau_\alpha(\phi; N)$ are fit to Eq. (2). (bottom). To obtain the universal scaling exponent of τ_α near $\phi_c(N)$, the fit was made using $\tau_\alpha/\tau_0(N) = (\phi_c(N) - \phi)^{-\nu_\tau}$ for all N, which confers $\nu_\tau = 0.65$. (c) Finite size scaling to obtain $\phi_c^\infty \equiv \phi_c(N \gg 1)$. $\phi_c(N)$ s fitted to $\phi_c(N) = \phi_c^\infty - aN^{-\nu'}$ give $\phi_c^\infty = 0.449$, $a = 0.552$, and $\nu' = 0.432$.

to the variance in $F_{q_{\max}}(t)$, can distinguish between the states below and above ϕ_c clearly. The fourth order dynamic susceptibility [23], used to quantify dynamic heterogeneity in structural glasses, is given by

$$\chi_4(t) = N[\langle F_{q_{\max}}(t)^2 \rangle - \langle F_{q_{\max}}(t) \rangle^2]. \tag{3}$$

The amplitude of $\chi_4(t)$, $\chi_4^{\max}$, increases with ϕ [Fig. 3(a)], and the divergence of $\chi_4^{\max}$ near $\phi_c(N)$ can be described using $\chi_4^{\max}(\phi; N) = \chi_4^o(N)[\phi_c(N) - \phi]^{-\nu_\chi}$. The scaling exponent for the dynamical arrest transition is found to be $\nu_\chi \approx 0.37$. In the $N \to \infty$ limit, $\phi_c^\infty = 0.44$ [Fig. 3(c)], which is consistent with the $\phi_c^\infty = 0.45$ from the analysis based on Eq. (2).

The significance of the key finding is that $\phi_c^\infty \approx 0.44$ becomes transparent by predicting the consequences for chromosome dynamics in various organisms. Without confinement or any special interactions mediated by proteins, the genome occupies a large volume $V \sim (4\pi/3)(R_g^o)^3$ with $R_g^o \approx l_p(N/g)^{3/5}$ ($l_p \approx 50$ nm $= g \times 0.34$ nm/bp, thus $g \approx 147$ bp). Given that the nuclear sizes are similar [$\sim\mathcal{O}(1)$ μm], there could be a large variation in the nuclear volume fraction for different organisms that have different genomic size, N.

(i) For bacteria ($N = 10^6$ bp), $R_g^o \approx 10$ μm is greater than the bacterial cell size ~ 1 μm. As 1 bp corresponds to 1 nm³ [35], the volume fraction for the bacterial genome is $\phi_{\text{bac}} = 1$ nm³/bp $\times 10^6$ bp/1 μm³ $= 10^{-3} \ll \phi_c^\infty$, implying that glassy effects are not relevant.
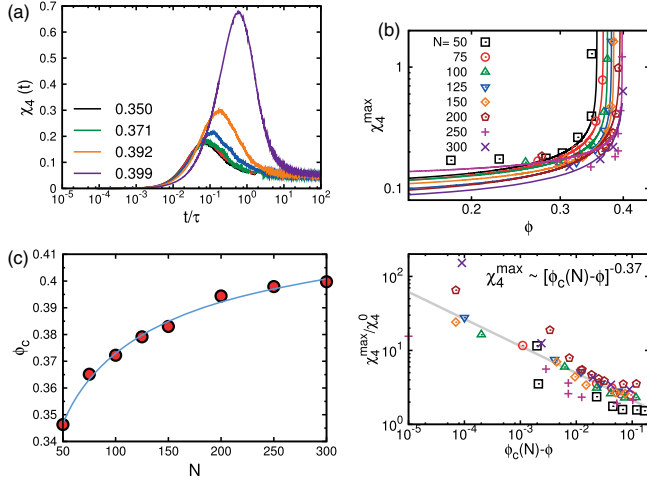
FIG. 3 (color online). Polymer dynamics under confinement probed using $\chi_4^{\max}(\phi)$. (a) $\chi_4^{\max}(t)$ with varying ϕ for $N = 300$. (b) (top) $\chi_4^{\max}(\phi) = \chi_4^o(N)(\phi_c(N) - \phi)^{-\nu_\chi}$ diverges at N-dependent critical volume fraction $\phi_c(N)$. (bottom) The data of τ_α are rescaled with $\tau_0(N)$ and the fit using $\chi_4^{\max}/\chi_4^o(N) = [\phi_c(N) - \phi]^{-\nu_\chi}$ for all N, which gives $\nu_\chi \approx 0.37$. (c) Finite size scaling: $\phi_c(N)$ fit to $\phi_c(N) = \phi_c^\infty - aN^{-\nu''}$ gives $\phi_c^\infty = 0.443$, $a = 0.571$, and $\nu'' = 0.453$. Note that $\nu' \approx \nu''$ [Fig. 2(c)].

(ii) In eukaryotes, DNA chains are organized in nucleosomes. Thus, it is more appropriate to estimate the volume of chromosomes in terms of the number of nucleosomes rather than the volume of bare DNA. Since each nucleosome, whose volume is $V_{\text{nuc}} \approx \pi \times 10^2 \times 3$ nm^3 (15–20 nm width, 2–3 nm height), is wrapped by ~ 150 bp DNA with a 50 bp-spacer between the neighboring nucleosomes [36], 200 bp-DNA is required to compose one nucleosome. For budding yeast $N \approx 10^8$ [37], the volume occupied by the entire nucleosomes is $V_{\text{gen}}^{\text{yeast}} = 10^8$ bp/200 bp $\times V_{\text{nuc}} \approx 0.47$ μm^3, and the yeast nucleus volume is $V_{\text{nucls}}^{\text{yeast}} \approx 4$ μm^3. Therefore, $\phi_{\text{yeast}} = V_{\text{gen}}^{\text{yeast}}/V_{\text{nucls}}^{\text{yeast}} \approx 0.12$, which is smaller than ϕ_c^∞. This explains the intrachromosomal contact frequency $P(s) \sim s^{-1.5}$ for the yeast genome, pointing to an equilibrium globule [8,38–40].

(iii) Human nucleus size varies depending on the cell type and the stage of development, which results in $P(s) \sim s^{-1.5}$ for stem cell and $P(s) \sim s^{-1.0}$ for a mature cell [9]. For illustrative purposes, we adopt the nucleus volume $V_{\text{nucls}}^{\text{human}} \approx 60$–$110$ μm^3 from the average size of a mammalian cell nucleus $2 \times R \approx 5$–6 μm [8,41]. Since the volume taken by the entire 46 chromosomes, as a diploid with $2 \times N \approx 2 \times 3 \times 10^9$ bp, is $V_{\text{gen}}^{\text{human}} = 6 \times 10^9$ bp/200 bp $\times V_{\text{nuc}} \approx 3 \times 10^{10}$ nm^3, the volume fraction of the human genome is $\phi_{\text{human}} = V_{\text{gen}}^{\text{human}}/V_{\text{nucls}}^{\text{human}} \approx 0.3$–$0.5 \gtrsim \phi_c^\infty$. Of particular note is that $\phi_{\text{human}} \gtrsim \phi_c^\infty$. Thus, the lack of nuclear space in the human cell makes the chromosome dynamics intrinsically glassy, indefinitely slowing down the relaxation of the chromosome configuration. This

crucial conclusion based on the simple estimate of ϕ_{human} suggests the decondensation-condensation process, driven by a panoply of partner enzymes, is likely to be under kinetic control.

(iv) The volume fraction of DNA ($L \approx 6$–60 μm) inside a viral capsid ($R \approx 25$–50 nm) using $L \sim 30$ μm and $R \sim 35$ nm is $\phi_{\text{virus}} \approx 0.5 > \phi_c$ [13,42]. A recent experiment showed that dynamics of viral packaging is ultraslow and glassy resulting in significant heterogeneity in packaging rates that vary from one virus to another [19]. It is noteworthy that the size of viral DNA $[N = (30 \times 10^3)/0.34 = 8.8 \times 10^4$ bp] is only $\sim 10\%$ of the bacterial genome. Thus, the equilibration time of DNA conformation based on reptation (or scaling) should occur 10^3 times faster than in bacterial genome, which would contradict experiments [19]. To explain the ultraslow and heterogeneous dynamics of viral DNA packaging it is essential to consider the effects of confinement, and our theory provides a natural explanation of the observations.

Our study provides a general framework to quantify glassy dynamics of a polymer chain (a simple model for chromosome organization) and highlights the nonequilibrium aspect of a single polymer under strong confinement with clear implications for the variations in genome folding across different species. The dynamical implication of our finding $\phi_{\text{bac}} \ll \phi_{\text{yeast}} < \phi_c^\infty \lesssim \phi_{\text{human}} < \phi_{\text{virus}}$, and the correlations of $\phi_{\text{yeast}} < \phi_c^\infty$ with $P(s) \sim s^{-1.5}$ for budding yeast [38] and $\phi_c^\infty \lesssim \phi_{\text{human}}$ with $P(s) \sim s^{-1}$ for mature human cells [9] provide a new framework for understanding the origin of qualitatively distinct chromosome organization in various organisms and cell types.

Given that the cellular environment is replete with crowding particles, the volume fractions estimated here for different organisms may well be only lower bounds, and thus we expect that glassy dynamics is prevalent especially in higher-order organisms. To overcome topological constraints, fluidization, or equilibration of the nuclear environment using topoisomerase or metabolic activity would be sometimes necessary for biological systems to execute their functions [43]. Furthermore, it is noteworthy that although there is not a significant difference in genome volume fraction between a human embryonic stem cell (HESC) and mature cell [44], these two cells have distinct $P(s)$ $[P(s) \sim s^{-1.5}$ for HESC, $P(s) \sim s^{-1.0}$ for a mature cell] [9,10], which may be linked to substantial variations in metabolic activity or specific interactions with the nuclear envelope depending on the cell maturity. Although our conclusions here do not consider the role of active mechanisms on genome organization, it is plausible that equilibration machineries exploiting active forces are required when chromosome dynamics is intrinsically glassy, as appears to be the case in higher organisms.

---

*hyeoncb@kias.re.kr

[1] T. Nagano, Y. Lubling, T. J. Stevens, S. Schoenfelder, E. Yaffe, W. Dean, E. D. Laue, A. Tanay, and P. Fraser, Nature (London) **502**, 59 (2013).

[2] T. Cremer and C. Cremer, Nat. Rev. Genet. **2**, 292 (2001).

[3] E. Lieberman-Aiden et al., Science **326**, 289 (2009).

[4] A. Bolzer et al., PLoS Biol. **3**, e157 (2005).

[5] J. Dekker, K. Rippe, M. Dekker, and N. Kleckner, Science **295**, 1306 (2002).

[6] S. S. Rao et al., Cell **159**, 1665 (2014).

[7] J. Dekker, M. A. Marti-Renom, and L. A. Mirny, Nat. Rev. Genet. **14**, 390 (2013).

[8] L. A. Mirny, Chromosome research : an international Journal on the molecular, supramolecular and evolutionary aspects of chromosome biology **19**, 37 (2011).

[9] M. Barbieri, M. Chotalia, J. Fraser, L.-M. Lavitas, J. Dostie, A. Pombo, and M. Nicodemi, Proc. Natl. Acad. Sci. U.S.A. **109**, 16173 (2012).

[10] B. Zhang and P. G. Wolynes, Proc. Natl. Acad. Sci. U.S.A. **112**, 6062 (2015).

[11] A. Grosberg, Y. Rabin, S. Havlin, and A. Neer, Europhys. Lett. **23**, 373 (1993).

[12] A. Rosa and R. Everaers, PLoS Comput. Biol. **4**, e1000153 (2008).

[13] J. D. Halverson, J. Smrek, K. Kremer, and A. Y. Grosberg, Rep. Prog. Phys. **77**, 022601 (2014).

[14] M. Müller, J. P. Wittmer, and M. E. Cates, Phys. Rev. E **61**, 4078 (2000).

[15] J. Mateos-Langerak et al., Proc. Natl. Acad. Sci. U.S.A. **106**, 3812 (2009).

[16] J. L. Sikarov and G. Jannink, Biophys. J. **66**, 827 (1994).

[17] P. G. de Gennes, Scaling Concepts in Polymer Physics (Cornell University Press, Ithaca and London, 1979).

[18] A. Yu. Grosberg, S. K. Nechaev, and E. I. Shakhnovich, J. Phys. **49**, 2095 (1988).

[19] Z. T. Berndsen, N. Keller, S. Grimes, P. J. Jardine, and D. E. Smith, Proc. Natl. Acad. Sci. U.S.A. **111**, 8345 (2014).

[20] T. B. Le, M. V. Imakaev, L. A. Mirny, and M. T. Laub, Science **342**, 731 (2013).

[21] N. Tokuda, T. P. Terada, and M. Sasai, Biophys. J. **102**, 296 (2012).

[22] N. Ganai, S. Sengupta, and G. I. Menon, Nucleic Acids Res. **42**, 4145 (2014).

[23] T. R. Kirkpatrick and D. Thirumalai, Phys. Rev. A **37**, 4439 (1988).

[24] H. Kang, T. R. Kirkpatrick, and D. Thirumalai, Phys. Rev. E **88**, 042308 (2013).

[25] T. R. Kirkpatrick and D. Thirumalai, Rev. Mod. Phys. **87**, 183 (2015).

[26] M. Daoud, J. P. Cotton, B. Farnoux, G. Jannink, G. Sarma, H. Benoit, R. Duplessix, C. Picot, and P. G. de Gennes, Macromolecules **8**, 804 (1975).

[27] A. Y. Grosberg and A. R. Khokhlov, Statistical Physics of Macromolecules (AIP Press, New York, 1994).

[28] A. Cacciuto and E. Luijten, Nano Lett. **6**, 901 (2006).

[29] See Supplemental Material at http://link.aps.org/supplemental/10.1103/PhysRevLett.115.198102 for the model and simulations, volume fraction of a confined polymer, definitions of $g(r)$ and $P(s)$, the relationship of $P(s) \sim s^{2.18}$ for unconfined SAW, and Supplemental figures.

[30] J. des Cloizeaux, J. Phys. **41**, 223 (1980).

[31] S. Redner, J. Phys. A **13**, 3525 (1980).

[32] N. Toan, P. Greg Morrison, C. Hyeon, and D. Thirumalai, J. Phys. Chem. B **112**, 6094 (2008).

[33] R. Lua, A. L. Borovinskiy, and A. Y. Grosberg, Polymer **45**, 717 (2004).

[34] G. Gürsoy, Y. Xu, A. L. Kenter, and J. Liang, Nucleic Acids Res. **42**, 8223 (2014).

[35] R. Phillips, J. Kondev, J. Theriot, N. Orme, and H. Garcia, Physical Biology of the Cell (Garland Science, New York, 2009).

[36] Z. Hui, Y. Zhang, S. B. Zhang, C. Jiang, Q. Y. He, M. Q. Li, and R. L. Qian, Cell Res. **9**, 255 (1999).

[37] A. Goffeau et al., Science **274**, 546 (1996).

[38] H. Wong, H. Marie-Nelly, S. Herbert, P. Carrivain, H. Blanc, R. Koszui, E. Fabre, and C. Zimmer, Curr. Biol. **22**, 1881 (2012).

[39] M. Emanuel, N. H. Radja, A. Henriksson, and H. Schiessel, Phys. Biol. **6**, 025008 (2009).

[40] P. Therizols, T. Duong, B. Dujon, C. Zimmer, and E. Fabre, Proc. Natl. Acad. Sci. U.S.A. **107**, 2025 (2010).

[41] B. Alberts, A. Johnson, J. Lewis, M. Raff, K. Roberts, and P. Walter, Molecular Biology of the Cell, 5th ed. (Garland Science, New York, 2008).

[42] P. K. Purohit, M. M. Inamdar, P. D. Grayson, T. M. Squires, J. Kondev, and R. Phillips, Biophys. J. **88**, 851 (2005).

[43] B. R. Parry, I. V. Surovtsev, M. T. Cabeen, C. S. O'Hern, E. R. Dufresne, and C. Jacobs-Wagner, Cell **156**, 183 (2014).

[44] S. Pagliara, K. Franze, C. R. McClain, G. W. Wylde, C. L. Fisher, R. J. Franklin, A. J. Kabla, U. F. Keyser, and K. J. Chalut, Nat. Mater. **13**, 638 (2014).